The controlled synthesis of nitrogen and iron co-doped $Ni_3S_2@NiP_2$ heterostructure for oxygen evolution reaction and urea oxidation reaction

Jiaxin Li[a], Hongyi Cui[a], Xiaoqiang Du[a*] and Xiaoshuang Zhang[b]

[a] School of Chemical Engineering and Technology, North University of China, Xueyuan road 3, Taiyuan 030051, People's Republic of China. E-mail: duxq16@nuc.edu.cn

[b] School of Science, North University of China, Xueyuan road 3, Taiyuan 030051, People's Republic of China.

Gas detection. The same volume of gas sample in the headspace of the electrolytic cell was withdrawn by a SGE gas-tight syringe and analyzed by gas chromatography (GC). The O_2 in the sampled gas was separated by passing through a 2 m × 3 mm packed molecular sieve 5A column with an Ar carrier gas and quantified by a Thermal Conductivity Detector (TCD) (Shimadzu GC-9A).

Turnover frequency (TOF) calculations: To calculate TOF, we need to calculate the surface concentration of active sites associated with the redox Ni species by electrochemistry. The linear relationship between the plot of the oxidation peak current densities for redox Ni species and scan rates can be derived from the electrochemical cyclic voltammetry scans according to the following equation:

Slope = $n^2F^2A\,\Gamma_0/RT$

Where n representing the number of electrons transferred is 1 assuming a one–electron process for oxidation of Ni centers in N-Fe-$Ni_3S_2@NiP_2$; F is Faraday's constant (96485 C mol^{-1}); A is the geometrical surface area of the electrode; Γ_0 is the surface concentration of active sites (mol cm^{-2}), and R and T are the ideal gas constant and the absolute temperature, respectively.

TOF values can be finally calculated based on the formula:

TOF = $jA/4Fm$

Where j is the current density, 4 indicate the mole of electrons consumed for one mole of O_2 evolution, and m is the mole number of active sites.

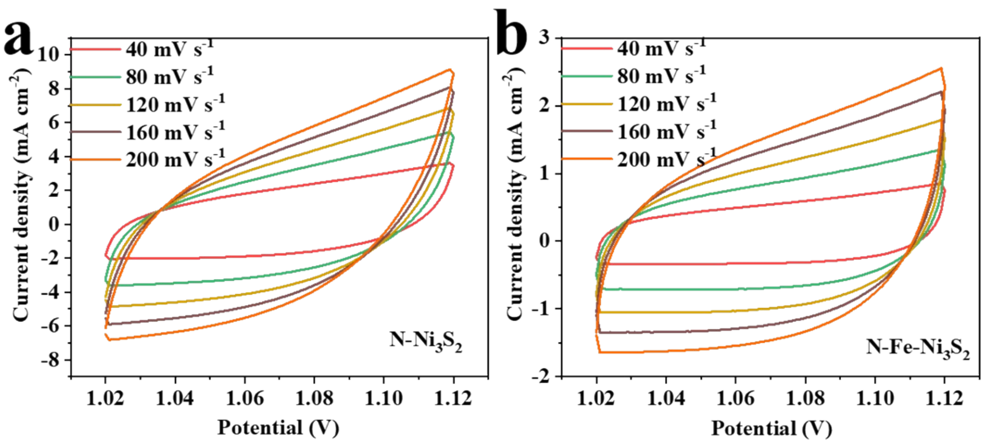

Fig. S1. CV of N-Ni_3S_2(a) and N-Fe-Ni_3S_2(b).

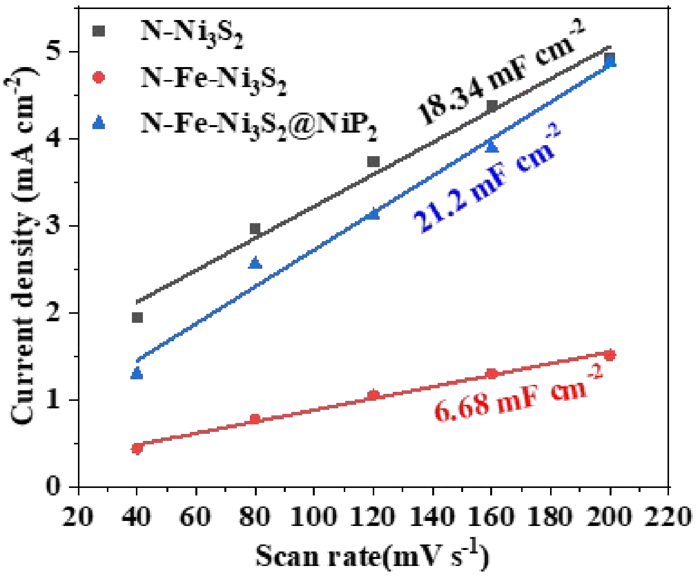

Fig. S2. The C_{dl} of $N\text{-}Ni_3S_2$, $N\text{-}Fe\text{-}Ni_3S_2$ and $N\text{-}Fe\text{-}Ni_3S_2@NiP_2$.

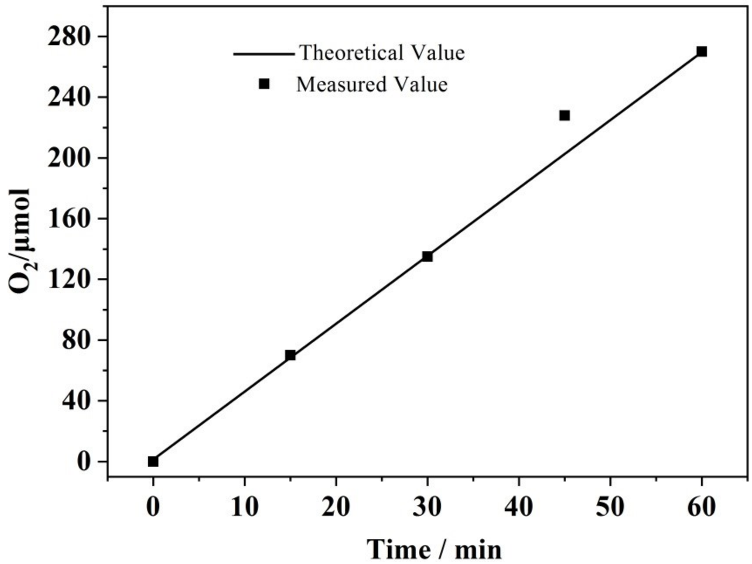

Fig. S3. Electrocatalytic efficiency of O_2 production over $N\text{-}Fe\text{-}Ni_3S_2@NiP_2/NF$.

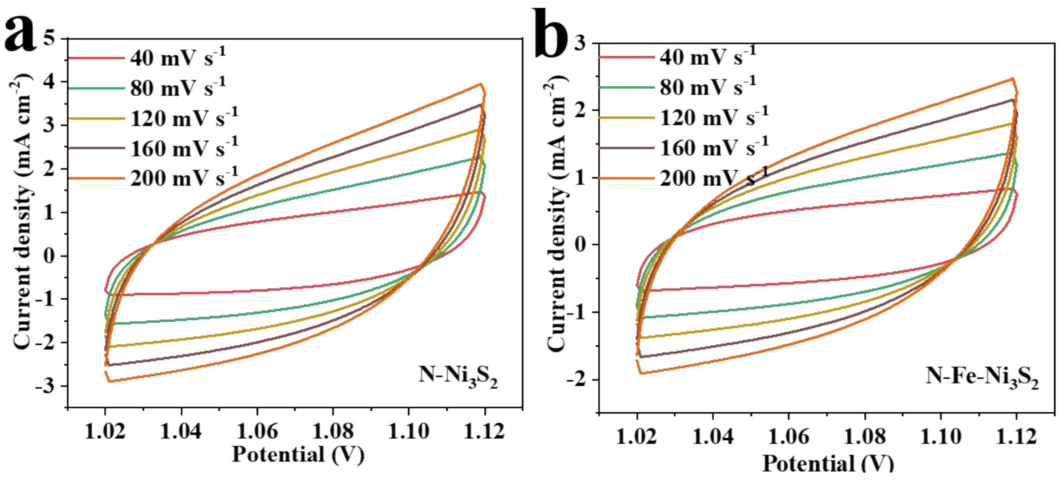

Fig. S4. CV of $N\text{-}Ni_3S_2$(a) and $N\text{-}Fe\text{-}Ni_3S_2$(b).

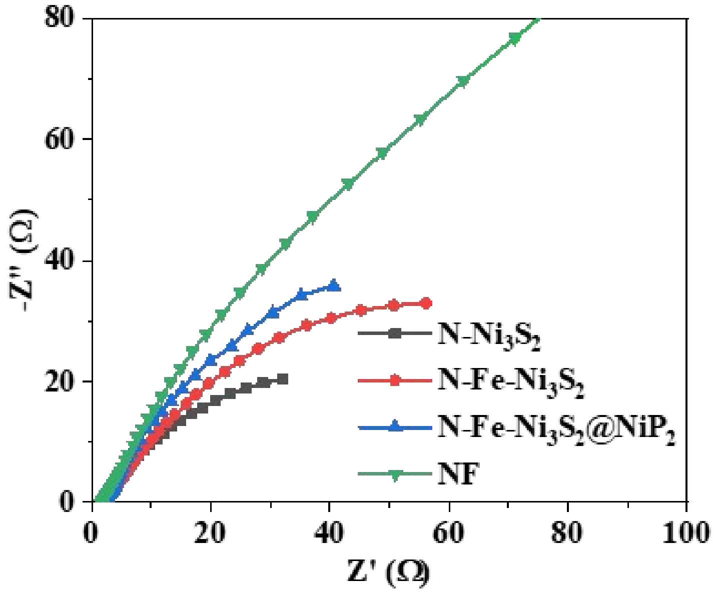

Fig. S5. Nyquist plots of the product.

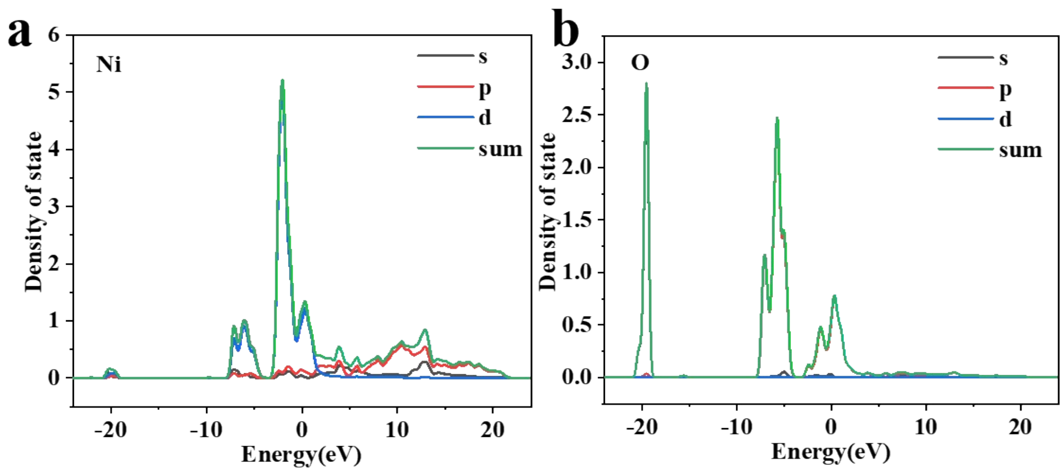

Fig. S6. Density of states for NiOOH, (a) Ni and (b) O.

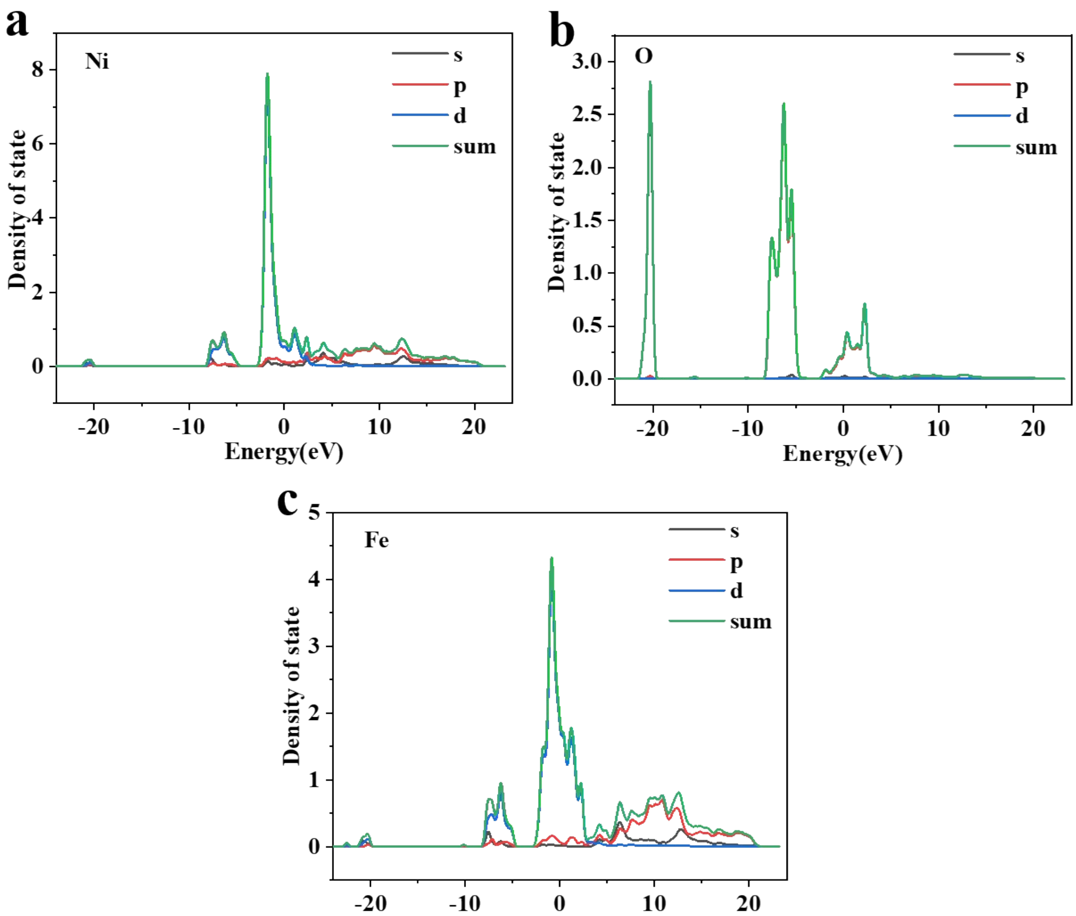

Fig. S7. Density of states for Fe-NiOOH, (a) Ni, (b) O and (c) Fe.

Table S1. Comparison of OER performances of reported electrocatalyst in 1.0 M KOH

Materials	η@10 mA cm^{-2} (mV)	η@100 mA cm^{-2} (mV)	Ref.
N-Fe-Ni_3S_2@NiP_2/NF	**--**	**251**	**This work**
N-Ni_3S_2/NF	--	330	[1]
Ni/NiS	--	~390	[2]
MoS_2/Ni_3S_2	218	~290	[3]
CoZnP/CNTs	281	--	[4]
Mn-Co oxyphosphide	320	~350	[5]
NiFe/N–C	--	300	[6]
NP-$Ni_{0.70}Fe_{0.30}$	260	320	[7]
CoFeCr LDH/NF	202	~320	[8]

Table S2. Comparison of UOR performances of reported electrocatalyst in 1.0 M KOH

Materials	Electrolyte 1 M KOH	η@100 mA cm^{-2} (V)	Ref.
N-Fe-Ni_3S_2@NiP_2/NF	**0.5 M urea**	**1.353**	**This work**
NF/MnO_2	0.5 M urea	1.45	[9]
$Ni_{0.975}Fe_{0.025}$-P@CC	0.5 M urea	1.38	[10]
Ni_3N/NF	0.5 M urea	1.4	[11]
$Fe_{11.1\%}$-Ni_3S_2/NF(array)	0.33 M urea	1.45	[12]
1% Cu:α-$Ni(OH)_2$/NF	0.33 M urea	1.41	[13]
MoS_2/Ni_3S_2/NiFe-LDH/NF	0.5 M urea	1.4	[14]
Mo–Co–S–Se/CC	0.5 M urea	1.41	[15]
NF/NiMoO-Ar	0.5 M urea	1.42	[16]

Notes and references

[1] P. Chen, T. Zhou, M. Zhang, Y. Tong, C. Zhong, N. Zhang, L. Zhang, C. Wu, Y. Xie, 3D Nitrogen-Anion-Decorated Nickel Sulfides for Highly Efficient Overall Water Splitting;Adv. Mater., 2017;29: 1701584.

[2] G.-F. Chen, T.Y. Ma, Z.-Q. Liu, N. Li, Y.-Z. Su, K. Davey, S.-Z. Qiao, Efficient and Stable Bifunctional Electrocatalysts Ni/NixMy (M = P, S) for Overall Water Splitting;Adv. Funct. Mater., 2016;26: 3314-23.

[3] J. Zhang, T. Wang, D. Pohl, B. Rellinghaus, R. Dong, S. Liu, X. Zhuang, X. Feng, Interface Engineering of MoS2/Ni3S2 Heterostructures for Highly Enhanced Electrochemical Overall-Water-Splitting Activity;Angewandte Chemie-International Edition, 2016;55: 6702-7.

[4] H. Xu, K. Zhang, C. Liu, L. Tian, Y. Du, 3D-1D Heterostructure of CoZn Oxyphosphide Nanosheets Anchored on Carbon Nanotubes as Electrocatalysts for the Oxygen Evolution Reaction;ChemElectroChem, 2018;5: 2558-63.

[5] B.Y. Guan, L. Yu, X.W. Lou, General Synthesis of Multishell Mixed-Metal Oxyphosphide Particles with Enhanced Electrocatalytic Activity in the Oxygen Evolution Reaction;Angewandte Chemie-International Edition, 2017;56: 2386-9.

[6] J. Zhang, F. Xing, H. Zhang, Y. Huang, Ultrafine NiFe clusters anchored on N-doped carbon as bifunctional electrocatalysts for efficient water and urea oxidation;Dalton Trans., 2020;49: 13962-9.

[7] Z. Cao, T. Zhou, X. Ma, Y. Shen, Q. Deng, W. Zhang, Y. Zhao, Hydrogen Production from Urea Sewage on NiFe-Based Porous Electrocatalysts;ACS Sustainable Chem. Eng., 2020;8: 11007-15.

[8] Z. Wang, W. Liu, Y. Hu, M. Guan, L. Xu, H. Li, J. Bao, H. Li, Cr-doped CoFe layered double hydroxides: Highly efficient and robust bifunctional electrocatalyst for the oxidation of water and urea;Appl. Catal., B, 2020;272: 118959.

[9] S. Chen, J. Duan, A. Vasileff, S.Z. Qiao, Size Fractionation of Two-Dimensional Sub-Nanometer Thin Manganese Dioxide Crystals towards Superior Urea Electrocatalytic Conversion;Angewandte Chemie-International Edition, 2016;55: 3804-8.

[10] T. Ma, Y. Qiu, Y. Zhang, X. Ji, P.-A. Hu, Iron-Doped Ni5P4 Ultrathin Nanoporous Nanosheets for Water Splitting and On-Demand Hydrogen Release via NaBH4 Hydrolysis;ACS Appl. Nano Mater., 2019;2: 3091-9.

[11] S. Hu, C. Feng, S. Wang, J. Liu, H. Wu, L. Zhang, J. Zhang, Ni3N/NF as Bifunctional Catalysts for Both Hydrogen Generation and Urea Decomposition;ACS Appl. Mater. Interfaces, 2019;11: 13168-75.

[12] W. Zhu, Z. Yue, W. Zhang, N. Hu, Z. Luo, M. Ren, Z. Xu, Z. Wei, Y. Suo, J. Wang, Wet-chemistry topotactic synthesis of bimetallic iron-nickel sulfide nanoarrays: an advanced and versatile catalyst for energy efficient overall water and urea electrolysis;J. Mater. Chem. A, 2018;6: 4346-53.

[13] J. Xie, L. Gao, S. Cao, W. Liu, F. Lei, P. Hao, X. Xia, B. Tang, Copper-incorporated hierarchical wire-on-sheet alpha-Ni(OH)(2) nanoarrays as robust trifunctional catalysts for synergistic hydrogen generation and urea oxidation;J. Mater. Chem. A, 2019;7: 13577-84.

[14] M. He, S. Hu, C. Feng, H. Wu, H. Liu, H. Mei, Interlaced rosette-like MoS2/Ni3S2/NiFe-LDH grown on nickel foam: A bifunctional electrocatalyst for hydrogen production by urea-assisted electrolysis;Int. J. Hydrogen Energy, 2020;45: 23-35.

[15] Z. Wu, X. Guo, Z. Zhang, M. Song, T. Jiao, Y. Zhu, J. Wang, X. Liu, Interface Engineering of MoS2 for Electrocatalytic Performance Optimization for Hydrogen Generation via Urea Electrolysis;ACS Sustainable Chem. Eng., 2019;7: 16577-84.

[16] Z.-Y. Yu, C.-C. Lang, M.-R. Gao, Y. Chen, Q.-Q. Fu, Y. Duan, S.-H. Yu, Ni-Mo-O nanorod-derived composite catalysts for efficient alkaline water-to-hydrogen conversion via urea

electrolysis;Energy Environ. Sci., 2018;11: 1890-7.